

## Understanding the reversible and irreversible deactivation of methane oxidation catalysts



Rasmus Lykke Mortensen <sup>a,b</sup>, Hendrik-David Noack <sup>b</sup>, Kim Pedersen <sup>b</sup>, Maja A. Dunstan <sup>a</sup>, Fabrice Wilhelm <sup>c</sup>, Andrei Rogalev <sup>c</sup>, Kasper S. Pedersen <sup>a</sup>, Jerrik Mielby <sup>a,\*</sup>, Susanne Mossin <sup>a,\*</sup>

<sup>a</sup> DTU Chemistry, Technical University of Denmark, Kemitorvet 207, DK-2800 Kgs. Lyngby, Denmark

<sup>b</sup> Umicore Denmark Aps, Kogle Allé 1, DK-2970 Hørsholm, Denmark

<sup>c</sup> ESRF – The European Synchrotron, BP 220, 38043 Grenoble Cedex 9, France

### ARTICLE INFO

Original content: [ESI\\_kinetic data.xlsx \(Original data\)](#)

#### Keywords:

Methane oxidation  
Palladium  
Deactivation  
Kinetic model  
CH<sub>4</sub>-TPR

### ABSTRACT

Catalytic oxidation is a promising technology for controlling methane emissions from natural gas engines, but fast and severe deactivation prevents implementation. We investigated a commercial Pd on alumina oxidation catalyst under realistic conditions and identified two deactivation phenomena: fast, reversible inhibition and slow, irreversible loss of active sites. The loss of active sites occurs only during methane conversion, fortunately a brief oxygen cut-off is enough to regenerate the catalyst. Both types of deactivation increase the reduction temperature of PdO. From 36 kinetic experiments we propose a simple kinetic model encompassing both types of deactivation. The inhibition is confirmed to be due to water coverage of the active sites whereas dispersion of Pd on the surface is the cause of the irreversible loss of active sites. The new insight shows a pathway toward designing more durable catalysts for complete methane oxidation.

### 1. Introduction

Although the combustion of liquid natural gas (LNG) emits less CO<sub>2</sub> than other fossil fuels, an effective system for controlling the methane slip from large natural gas engines is needed to decrease the total environmental impact. Since the global warming potential of CH<sub>4</sub> is around 81 times higher than CO<sub>2</sub> on a 20-year term (GWP<sub>20</sub> = 81.1), the most promising solution to control the emissions is to convert the CH<sub>4</sub> into CO<sub>2</sub> by complete catalytic oxidation. Unfortunately, fast and severe deactivation of the oxidation catalysts at relevant conditions remains a significant challenge that prevents commercial applications. It is well-known that there are several contributions to the decrease in activity of methane oxidation catalysts; water from the combustion process, sintering of active nanoparticles and SO<sub>2</sub>-poisoning all contribute in different ways. SO<sub>2</sub> and water acting together are especially detrimental [1]. Sintering can be diminished with the right choice of support and SO<sub>2</sub> can be avoided to some extent using clean fuel streams, but the water is a product in the combustion and a high content of water cannot be avoided.

Despite recent advances in developing catalysts with strong metal support interactions and hydrophobic supports [2–6], the water-induced

deactivation is still not fully understood. Pd is among the most active metals for complete methane oxidation, and the prevailing hypothesis is that the water forms hydroxyl groups on the surface of the active PdO [5, 7–13]. For example, Ciuparu et al. used in-situ diffuse reflectance infrared Fourier transform spectroscopy (DRIFTS) to show that more hydroxyl groups formed on a Pd/Al<sub>2</sub>O<sub>3</sub> catalyst under simulated wet methane oxidation than under similar conditions without methane [11]. More recently, Li et al. showed the existence of a PdOH phase on the surface of a palladium foil during simulated wet methane oxidation using ambient pressure X-ray photoelectron spectroscopy (XPS) [7]. Formation of Pd(OH)<sub>2</sub> after long term exposure to water has been suggested, but it has also been pointed out that this should not be stable at typical reaction temperatures and rather the formation of hydroxyls should be limited to the surface [14].

Several research groups have shown that introducing short reducing pulses (SRPs) is an effective way to restore the catalytic activity and maintain a high conversion of methane over time [15–18]. In a typical research setup, this is possible by shutting off the oxygen for a few seconds and allow the methane to quickly reduce Pd<sup>2+</sup> to Pd<sup>0</sup>. After exposure to oxidizing conditions, the regenerated catalyst becomes as active as the fresh catalyst, sometimes even more active. Based on

\* Correspondence to: DTU Chemistry, Technical University of Denmark, Kemitorvet 207, DK-2800 Kgs Lyngby.

E-mail addresses: [jjmie@kemi.dtu.dk](mailto:jjmie@kemi.dtu.dk) (J. Mielby), [slmo@kemi.dtu.dk](mailto:slmo@kemi.dtu.dk) (S. Mossin).

kinetic models and time-dependent X-ray absorption spectroscopy (XAS) data, Ferri et al. [17] showed that repeated SRPs could keep the supported palladium in a highly active state and suggested that the high catalytic activity relied on creating particles of amorphous  $\text{PdO}_x$  in contact with metallic Pd that acted as a reservoir for defects. The authors suggested that as the highly active and disordered  $\text{PdO}_x$  converted methane, it slowly crystallized into dense PdO, which has a lower catalytic activity. The active surface sites were proposed to be less crystalline because the PdO is coordinately unsaturated or contains some defects [19,20].

So far, there has been no consensus or positive identification of the deactivated phase. Surface OH groups and a dense PdO phase would be mutually exclusive descriptions of the irreversibly deactivated phase. Here we present the investigation of an efficient  $\text{Pd}/\text{Al}_2\text{O}_3$  oxidation catalyst under realistic operation conditions using primarily the catalytic test setup as the tool of investigation. The deactivation process is investigated by kinetic experiments monitored by the conversion of methane in a plug-flow reactor. We show for the first time that the two types of deactivation phenomena [12] have significantly different dependences on the partial pressures of water and that the irreversible deactivation depends on the conversion of methane. The catalytic setup was also optimized for measuring  $\text{CH}_4$ -TPR and a methodology was developed to run long experiments in series with excellent reproducibility. It was shown that both types of deactivation increase the reduction temperature of the active  $\text{Pd}^{2+}$ . In fact, the reduction temperature in  $\text{CH}_4$ -TPR was an excellent descriptor for the catalytic activity for both phenomena. The results of the  $\text{CH}_4$ -TPR investigation and ex-situ Pd L<sub>3</sub> X-ray absorption spectroscopy data showed that the deactivation was connected to dispersion and capture of Pd on the surface of the support under wet conditions.

## 2. Experimental

### 2.1. Material

Commercial dried and calcined  $\text{PdO}/\text{Al}_2\text{O}_3$  catalyst (Umicore Denmark Aps). The palladium content of the catalyst was determined to be 2.4 wt% with inductively coupled plasma optical emission spectrometry (ICP-OES) on a Varian Agilent 725-ES spectrometer. The sample was prepared for injection by acid digestion.

### 2.2. Catalytic testing

Complete methane oxidation reactions were conducted using a quartz fixed-bed reactor with an inner diameter of 10 mm. The reactor was positioned in a temperature-controlled furnace and fitted with a thermocouple inside the reactor just after the bed. The catalyst was ground, pressed, and crushed into particles ranging from 150 to 300  $\mu\text{m}$ . The bed was diluted with 2 g  $\text{SiO}_2$  sand (150–300  $\mu\text{m}$ ) for experiments with 200 mg catalyst, and with 1 g for experiments with 20 and 5 mg catalyst. The bed was positioned on a quartz wool plug and 500 mg quartz sand to get a level base. Four gasses were fed by independent mass flow controllers from Bronkhorst: Air,  $\text{N}_2$ ,  $\text{CO}_2$ , and 2%  $\text{CH}_4$  in  $\text{N}_2$  with a total flow rate of 420 ml/min. Steam was added to the gas stream by a Controlled Evaporator-Mixer (CEM, Bronkhorst), which was fed by a stainless steel water container pressurized by  $\text{N}_2$ . The reactor was pressurized by an Equinilibar LF Series Precision Back Pressure Regulator. Feed and outlet methane partial pressure was measured using a Thermo-FID ES from SK Elektronik and conversion calculated as:

$$\text{Conversion} = \frac{p(\text{CH}_4)_{\text{in}} - p(\text{CH}_4)_{\text{out}}}{p(\text{CH}_4)_{\text{in}}}$$

Where  $p(\text{CH}_4)_{\text{in}}$  and  $p(\text{CH}_4)_{\text{out}}$  are the methane gas partial pressures in the inlet and outlet gas, respectively. Light-off tests were performed at a ramp of  $\pm 5$   $^{\circ}\text{C}/\text{min}$ . Data displayed from these tests were collected

while the temperature was ramped down unless stated otherwise. Catalyst regeneration consisting of a short reducing pulse was conducted in the same catalytic setup. It was performed by exposing the reactor bed to 1000 ppm  $\text{CH}_4$  in  $\text{N}_2$  in a total gas flow of 380 ml/min for 5 min followed by reoxidation for 10 min at 1000 ppm  $\text{CH}_4$ , 10%  $\text{O}_2$  in  $\text{N}_2$  at 440 ml/min. Prior to kinetic experiments, using fresh catalyst beds every time, the catalyst was degreed for 1 h at 500  $^{\circ}\text{C}$  in the same gas mixture.

### 2.3. $\text{CH}_4$ -TPR

Methane temperature programmed reduction ( $\text{CH}_4$ -TPR) experiments were performed in the same reactor setup as the catalytic testing. The sample was placed on a plug of quartz wool leveled off by 500 mg  $\text{SiO}_2$  sand. After a deactivation segment, the flow was changed to dry  $\text{N}_2$  and the sample was flushed for 1 h at 420  $^{\circ}\text{C}$  and cooled down in preparation for TPR. Slight changes in the experimental parameters compared to the catalytic testing experiments were implemented to achieve high-quality TPR data: Signal-to-noise ratio of the FID detector output was maximized by running at low partial pressure of methane (500 ppm). Peak sharpness was improved by ramping at a low rate of 2.5  $^{\circ}\text{C}/\text{min}$ . Catalyst samples were undiluted to ensure a short bed and thereby minimal thermal variation across the length of the bed.

The TPR experiment served as the reducing part of a regeneration. Therefore, multiple experiments consisting of deactivation followed by TPR could be performed on the same bed, see [Supplementary Material](#) for further details.

### 2.4. XAS

Pd L<sub>3</sub>-edge X-ray absorption spectroscopy (XAS) experiment was performed at the ID12 beamline at the European Synchrotron Radiation Facility (Grenoble, France). Samples were restrained in mineral oil and kapton foil and spectra were measured at room temperature using total fluorescence yield detection mode. The catalyst material was measured in the fresh state and after having been exposed to a 60 h deactivation in 1000 ppm  $\text{CH}_4$ , 10% water and then flushed with  $\text{N}_2$  and cooled down using the same procedure as described for TPR above. Pristine PdO powder was measured at the same experimental conditions. The absorbance of the first photon energy scan was normalized to zero absorbance before the edge and to unity well above the edge (3195 eV). The spectrum of the PdO was corrected for self-absorption. Due to the close proximity in energy of the Pd L<sub>2</sub> edge an EXAFS analysis was not performed. The white line integral was calculated by first subtracting an arctan function from the data and then fitting the resulting line shape to a gaussian function and integrating the area [21].

## 3. Results

To study the effect of water on the deactivation of PdO for complete methane oxidation, we needed a catalyst with high activity at dry conditions which was based on a stable support material designed to withstand challenging reaction conditions. We chose a commercial catalyst, PdO supported on high surface  $\text{Al}_2\text{O}_3$  supplied by Umicore. Long-term stability tests were performed in a quartz fixed-bed reactor at high space velocity in a simulated engine exhaust, with realistic low methane content, 100–2500 ppm, different water content up to 20 vol %, 5 vol%  $\text{CO}_2$  and 10 vol%  $\text{O}_2$ . Care was taken to dilute the catalyst bed well to keep a homogeneous temperature in the bed even at high conversion. The methane conversion was determined with high sensitivity using an FID detector.

[Fig. 1](#) shows the methane conversion versus time at 440  $^{\circ}\text{C}$  with 500 ppm  $\text{CH}_4$  and 10%  $\text{O}_2$ , adding water (10 vol%) to the feed at 20 min and removing it again at 120 min. Under dry conditions, the methane conversion was stable at 94%, but after adding water, the conversion quickly dropped to 60% and decreased further over time. Upon

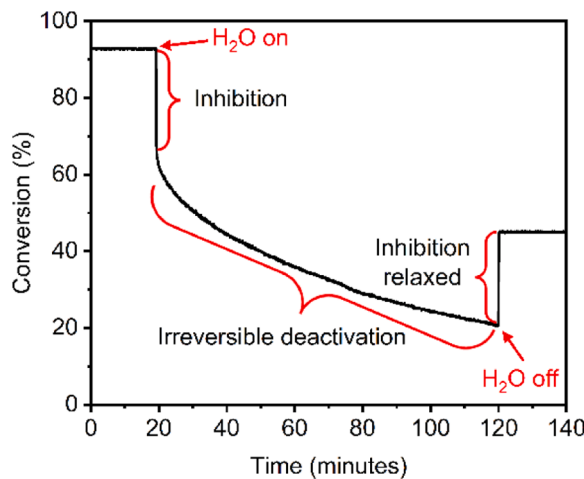


**Fig. 1.** Deactivation profile caused by water during complete methane oxidation by PdO/Al<sub>2</sub>O<sub>3</sub>. Reaction conditions: 500 ppm CH<sub>4</sub>, 10% O<sub>2</sub>, 10% H<sub>2</sub>O (when present), N<sub>2</sub> balance, T = 440 °C, WHSV = 1,260,000 ml h<sup>-1</sup> g<sup>-1</sup>.

removing the water from the feed, the methane conversion immediately increased to a new constant level. The decrease in conversion rate during the initial fast drop (measured in % of the rate before the change in conditions) is the same as the increase in conversion rate as water is turned off. This experiment shows the two separate processes taking place: Inhibition by water is fast and fully reversible [22], whereas a slow deactivation takes place over time and is irreversible under oxidizing reaction conditions. Since the catalyst could be regenerated using a simple reduction procedure (SRP at 440 °C, 500 ppm CH<sub>4</sub>), see Fig. S1, which resulted in a highly active and completely reproducible state, the so-called irreversible deactivation is only irreversible under oxidizing conditions, i.e. lean operation of an engine. We note that the freshly regenerated catalyst was even more active than the fresh catalyst, which is in good agreement with the literature, see Fig. S2 [17,18].

The fast inhibition is caused by adsorbed water or the formation of hydroxyl groups that block the active sites on the surface of PdO. It has been well characterized and discussed in the literature, a few examples being [13,23,24]. The deactivation with time, however, has been investigated in much less detail. Long-term experiments over several hours are only few in number [13] and the slow deactivation over time has not been characterized or understood well.

To investigate the interplay between water and methane during the reaction further, we designed several experiments to follow the conversion of methane during shifts in the feed, see Figs. 2 and S3. In the red trace in Fig. 2, water and oxygen were constantly fed to the catalyst whereas methane was only on for 5 min every 4 h. The black trace is the control experiment with constant methane feed. The catalyst quickly deactivated during the 5 min sampling time when methane was on, but the total deactivation was significantly less than in the control experiment despite the identical amount of water fed to the sample throughout the two experiments.

A model in which the deactivation rate is independent of the partial pressure of methane [13] would predict the same degree of deactivation in the two experiments, which is clearly not the case. Fig. S3 shows the results of changing the water content in the feed during an experiment and how the exact amount of water determined the deactivation rate even though the water content was always orders of magnitude higher than the methane content.

From these experiments we concluded that the currently accepted hypothesis for water-induced deactivation was not sufficient. Methane plays a key role in the irreversible loss of active surface sites. There are two possible explanations: 1) the presence of methane is causing the deactivation, or 2) the conversion of methane is causing the deactivation. To distinguish the two, we determined the conversion of the fresh

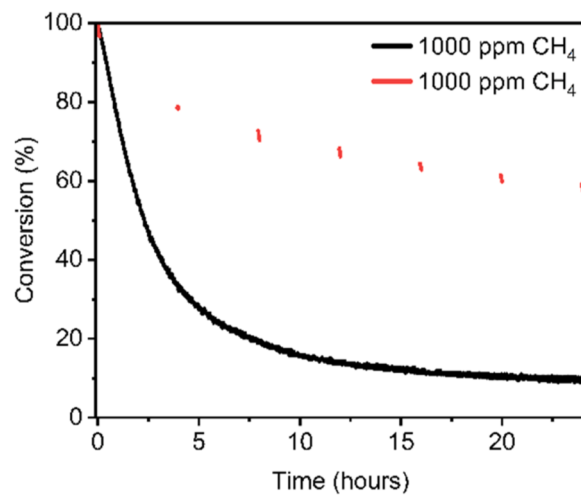


**Fig. 2.** Conversion of methane over long time. Black trace: Methane, oxygen and water are all fed continuously. Red trace: Oxygen and water are fed continuously but methane is only fed during 5 min intervals every 4 h to monitor the conversion level. Reaction conditions: 1000 ppm CH<sub>4</sub> (when present), 10% O<sub>2</sub>, 10% H<sub>2</sub>O, N<sub>2</sub> balance, T = 380 °C, WHSV = 126,000 ml h<sup>-1</sup> g<sup>-1</sup>.

catalyst in a typical light-off experiment under dry conditions and then exposed it to wet methane oxidation conditions for 24 h at two different temperatures. In experiment A, the temperature was 400 °C, which resulted in a decrease from > 99% to 15% conversion. In experiment B, the temperature was 250 °C and methane was barely converted (<1% conversion). The catalytic activity was checked in the same way after the exposure period, see Fig. 3. The results showed that the catalyst exposed at 400 °C required a higher temperature to reach 50% conversion ( $T_{50} = 288$  °C) than the catalyst exposed at 250 °C ( $T_{50} = 248$  °C). The increase was 61 °C and 21 °C, respectively. Water adsorption alone cannot explain this difference since more water adsorbs on the catalyst at low temperatures. Instead, these results indicate that the conversion of methane is causing the slow and irreversible loss of surface-active sites at wet conditions.

### 3.1. Kinetic experiments

Modeling the conversion profile of a reaction at different conditions helps decide which components of the reaction gases influence the reaction rates. This is useful information towards understanding the underlying mechanism and we proceeded to characterize the deactivation in this way. We performed 36 experiments at six different partial pressures of methane (100, 200, 500, 1000, 1750, and 2500 ppm) and six different partial pressures of water (0, 1, 2, 5, 10, and 15 vol%). In each experiment, the sample was degassed at 500 °C, then cooled down and water turned on at 380 °C for 2 min. Then, we stopped the water and increased the temperature to 440 °C, added the water once more, and followed the CH<sub>4</sub> conversion over the next 2 h. See the Supplementary Material for an example experiment, Fig. S4 and a detailed description of the experimental protocol.

The rate,  $r$ , at a given time in the experiment is calculated as

$$r = \frac{F \cdot p(\text{CH}_4)}{m_{\text{cat}}} \cdot \ln(1 - X)$$

where  $F$  is the total molar flow (mol s<sup>-1</sup>),  $p(\text{CH}_4)$  is the partial pressure of methane in the feed (measured in bar),  $m_{\text{cat}}$  is the mass of the catalyst (kg), and  $X$  is the fractional conversion.

The rate of methane conversion 1 min after turning on the water at 380 °C and 1 min and 1 h after turning on the water at 440 °C are plotted in a double logarithmic plot versus the methane partial pressure

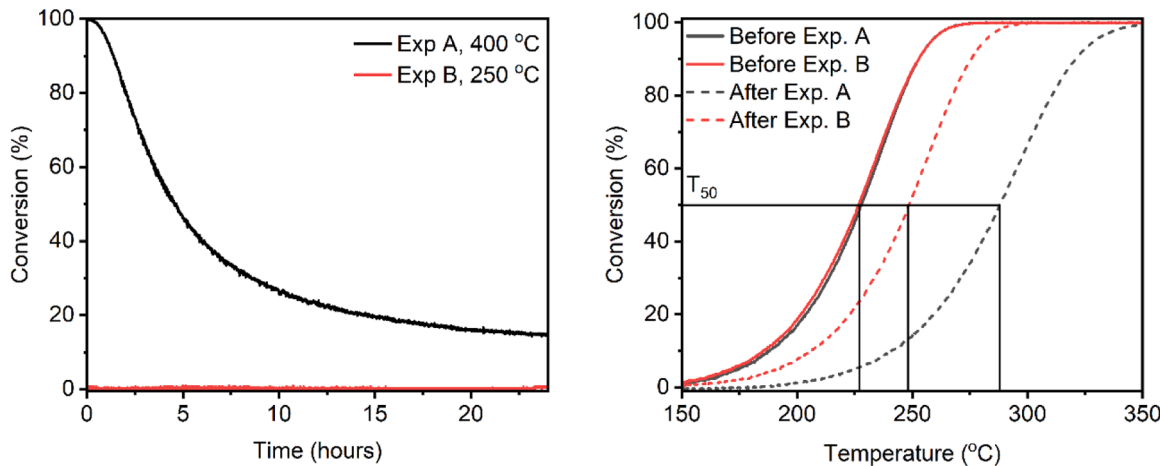


**Fig. 3.** Left: Conversion of methane as a function of the time-on-stream at 400 °C (Exp. A) and 250 °C (Exp. B), respectively. Right: Light-off experiments (ramping down) that show the catalytic activity before and after Exp. A and Exp. B. Reaction conditions during deactivation: 1000 ppm CH<sub>4</sub>, 10% O<sub>2</sub>, 10% H<sub>2</sub>O, N<sub>2</sub> balance, WHSV = 126,000 ml h<sup>-1</sup> g<sup>-1</sup>. Reaction conditions for light-off tests: 1000 ppm CH<sub>4</sub>, 10% O<sub>2</sub>, N<sub>2</sub> balance, ramp = 5 °C/min, WHSV = 126,000 ml h<sup>-1</sup> g<sup>-1</sup>.

and the water partial pressure, respectively, see Fig. S5. This type of plot is often used to determine the reaction order in reactants and products, here methane and water and are usually most reliable when measuring at differential conditions (low conversion) which was not always the case here. Nevertheless, with these reservations, it works quite well for the rate dependence on the methane concentration for the data points after inhibition. The reaction order in methane is determined to be 0.76 (7) at 380 °C and 0.85(5) at 440 °C. A few other values can be extracted from almost linear data: The reaction order in methane is unchanged

after 1 h on stream without water. The reaction order in water is around –1.0 after 1 h deactivation in water for high concentration of methane. The remaining plots all suffer from the data being not linear. The model especially suffers at high water content, and we proceeded to find better descriptors.

The result given in Fig. 1 and the fact that the rate decrease upon turning water on and the rate increase upon removing the water are identical show to us that treating the inhibition and the time-dependent deactivation as two separate phenomena are justified and that the

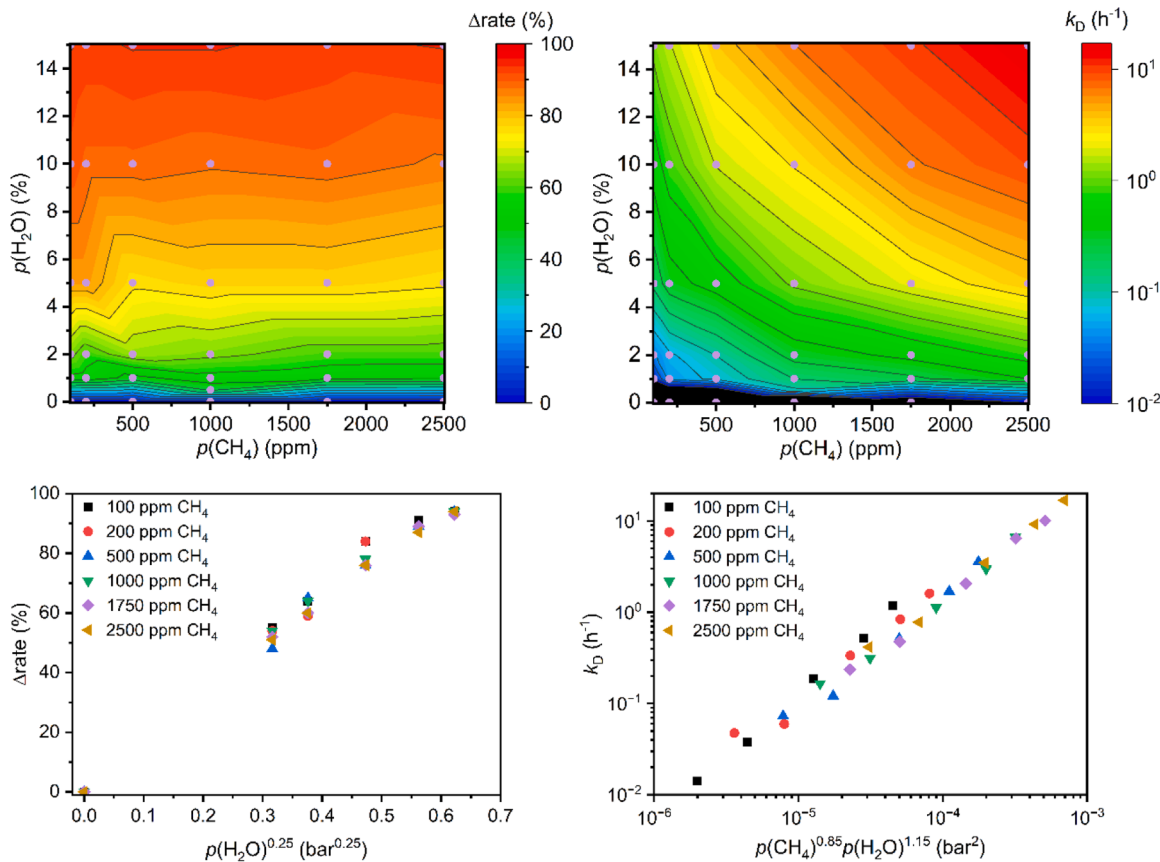


**Fig. 4.** Top left: Contour plot showing the decrease in reaction rate,  $\Delta\text{rate}$ , just after adding water at 380 °C as a function of the partial pressure of CH<sub>4</sub> and H<sub>2</sub>O (total pressure is 1 bar). Top right: Contour plot showing the second order rate coefficient for the slow and irreversible deactivation,  $k_D$ , as a function of  $p(\text{CH}_4)$  and  $p(\text{H}_2\text{O})$ . Bottom left:  $\Delta\text{rate}$ , plotted against  $p(\text{H}_2\text{O})^{0.25}$  for all partial pressures of CH<sub>4</sub>. Bottom right:  $k_D$  plotted against the product  $p(\text{H}_2\text{O})^{1.15} \cdot p(\text{CH}_4)^{1.15}$ .

change in reaction rate is a good descriptor for the inhibition just after water addition.

The decrease in rate during inhibition is calculated as:

$$\Delta\text{rate} = \frac{r_1 - r_2}{r_1} \cdot 100\%$$

where  $r_1$  and  $r_2$  are the reaction rates right before and 20 s after water addition. We use data at 380 °C for the modelling of the inhibition since the relative decrease in rate is better determined when the upper level is well away from 100% conversion. The data at 440 °C gives similar results but are less reliable due to the dry conversion being very close to 100%.

For the slow deactivation we find that we can model the data equally well with a first or with a second order rate expression at low water content. At high water content, however, the fit to the second-order rate expression is significantly better, see Fig. S6. For this reason, we use the second-order rate expression to fit the conversion versus time data at 440 °C from 30 s after the water was added:

$$\frac{1}{X(t)} = \frac{1}{X_0} + k_D t$$

where  $X(t)$  is the conversion at the time  $t$  (h),  $X_0$  is the initial conversion after the addition of water, and  $k_D$  is the deactivation rate coefficient, selected as the descriptor for the slow deactivation. Fig. 4 shows the 36 values for  $\Delta\text{rate}$  and  $k_D$  given as a function of the methane and water partial pressures in two contour plots. Notably, the fast inhibition only depends on the partial pressure of water. In contrast, the slow and irreversible deactivation depends on both the partial pressure of water and the partial pressure of methane.

The data in Fig. 4 bottom left and in Fig. S7 left agree well with the data of Keller et al. [25] who reported the effect of water on methane oxidation over PdO/Al<sub>2</sub>O<sub>3</sub> as measured by the difference in  $T_{50}$  and  $T_{100}$  in light-off experiments. [25] The effect of water does not reach a plateau, see Fig. S7 right. Higher water content continues to block more active sites [26,27].

### 3.2. Influence of temperature and pressure

Considering the potential application and reaction conditions inside a combustion engine, we also investigated the two deactivation phenomena at higher temperature and pressure, see Figs. S8-S11. The water causes more deactivation at lower temperatures. Above 450 °C, both types of deactivation are less pronounced, and at 575 °C the effect is almost gone. These observations agree well with the previous reports that describe the build-up of hydroxyl groups as the leading cause of deactivation [6,13]. Increasing the pressure to 2, 3, or 4 bar influences the conversion. As expected, the increase in pressure increases the residence time, which results in a higher reaction rate under dry conditions. The methane reaction rates are relatively similar under different pressures just after adding water to the feed. These results suggest that the increased inhibition by water as water is pushed onto the catalyst counteracts the increased activity caused by the higher residence time. For the slow deactivation, we observe that the deactivation rate coefficient increases significantly when we increase the pressure from 1 to 2 and 3 bar.

### 3.3. CH<sub>4</sub>-TPR experiments

To investigate the relationship between the two types of deactivations in more detail, we performed methane temperature-programmed reduction (TPR) experiments using 500 ppm CH<sub>4</sub> under dry conditions. During the TPR experiment, CH<sub>4</sub> reduced the PdO, which served the same purpose as reducing in an SRP. This procedure allowed us to run several experiments in series. After a short exposure to methane oxidation conditions to reoxidize and reset the catalytic

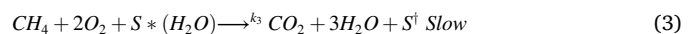
activity, we flushed and cooled the catalyst under nitrogen before the next run. Testing the reproducibility of the CH<sub>4</sub>-TPR after reduction and reoxidation always resulted in exactly the same reduction peak at 195 °C, see Fig. S12. A background reaction, most likely methane steam reforming or methane cracking [5] started to occur with increasing temperature. This contribution to the methane conversion was the same in all experiments and, therefore, disregarded in the TPR analysis.

The influence of water was investigated in two different experimental protocols performed on freshly regenerated catalysts: Fig. 5 left shows the influence of the water content during a 2 h pretreatment. With the increasing content of water, the sharp TPR peak gradually shifts towards higher temperatures. Furthermore, a small new peak appears at 265 °C. Fig. 5 right shows the influence of the time on stream in a pretreatment with 5% water. Already after 10 min pretreatment, the TPR-peak starts to broaden and shift towards a higher reduction temperature. The new peak at 265 °C also shifts with the pretreatment time. After 30 h, the original TPR peak is completely replaced by two peaks at 250 and 290 °C, respectively. The peak at 250 °C first appears between 10 and 30 h whereas the peak at 290 °C can be traced back to the 265 °C peak. Both peaks move to even higher temperatures when increasing pretreatment times. By subtracting the contribution from the constant background reaction, we find that the total area under the reduction peaks are the same in every experiment within the expected uncertainty, see Fig. S13. Furthermore, the amount of methane converted always corresponds to the reduction of 100% of the Pd present as determined by inductively coupled plasma optical emission spectrometry (ICP-OES). These results indicate that all the palladium is present as Pd<sup>2+</sup> in the beginning of the TPR experiments, and that the slow and irreversible deactivation changes the nature of the originally uniform PdO phase into a new type of Pd<sup>2+</sup> phase giving two separate reduction peaks. After 90 h on stream, the two reduction peaks are shifted by 65 and 103 °C compared to the freshly regenerated catalyst, respectively.

van Bokhoven et al. [28] and Cargnello et al. [29] recently showed that the presence of water changes the redox activity of Pd/Al<sub>2</sub>O<sub>3</sub> during methane oxidation. Inspired by these results, we designed a CH<sub>4</sub>-TPR experiment, where we added different partial pressures of water during the TPR analysis of freshly regenerated samples, see Fig. 6 left. Since Pd<sup>0</sup> on our catalyst catalyzes the steam reforming reaction (conversion of CH<sub>4</sub> and H<sub>2</sub>O into CO and H<sub>2</sub>), this reaction starts to occur as soon as the first PdO is reduced. Consequently, the reduction peak is not well shaped. Nevertheless, the sharp edge of the light-off temperature serves the same purpose as the peak in a typical TPR experiment. Fig. 6 right shows that the shift of the edge position in the wet CH<sub>4</sub>-TPR experiment relative to the dry experiment follows closely the initial rate loss during the fast inhibition as a function of the water content.

### 3.4. Kinetic modelling

To summarize, our results show that the deactivation of Pd<sup>2+</sup> during methane oxidation is caused by a fast and reversible inhibition and a slow and irreversible deactivation (loss of active sites) and that the two effects should be treated separately. Inhibition is a reversible equilibrium that increases with the partial pressure of water present, even with more than 20% water in the feed. In contrast, the slow deactivation is an irreversible phenomenon that only occurs if methane is converted under oxidizing conditions. To explain these key observations, we propose the following three equations:



Eq. 1 is the reaction of CH<sub>4</sub> with O<sub>2</sub> to give CO<sub>2</sub> and H<sub>2</sub>O. The reaction occurs on a site S that is unchanged by the reaction. Eq. 2 is the

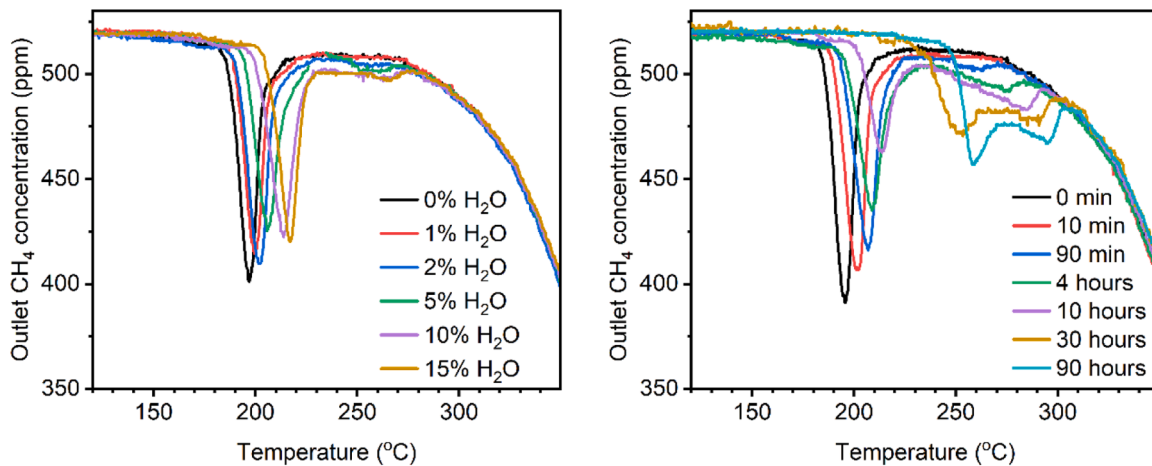


**Fig. 5.** CH<sub>4</sub>-TPR analysis (500 ppm CH<sub>4</sub> in N<sub>2</sub>, 2.5 °C/min, GHSV = 111,000 ml h<sup>-1</sup> g<sup>-1</sup>) performed after different pretreatments: Left: 2 h pretreatment with different partial pressures of water in the feed. Right: Different duration of the pretreatment with 5% water in the feed.

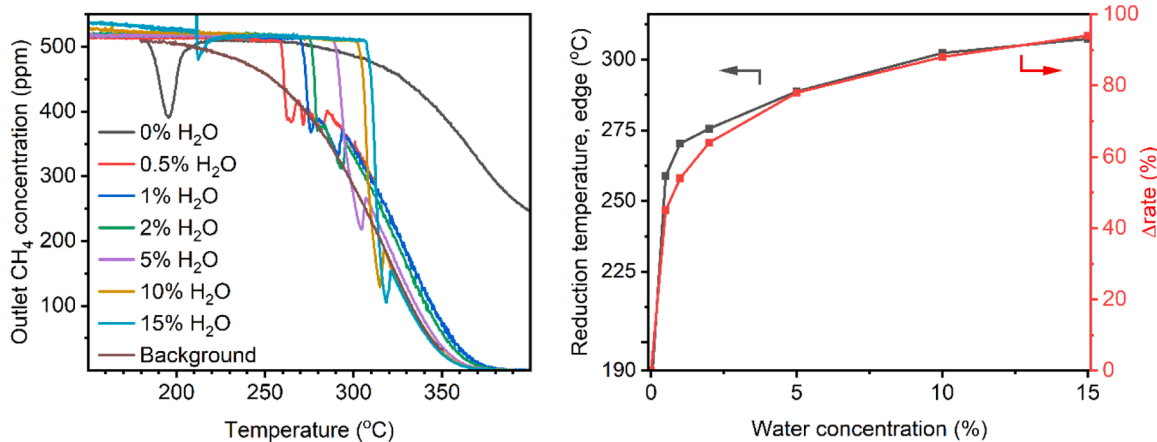


**Fig. 6.** Left: CH<sub>4</sub>-TPR (500 ppm CH<sub>4</sub> in N<sub>2</sub>, 2.5 °C/min, GHSV = 111,000 ml h<sup>-1</sup> g<sup>-1</sup>) performed in the presence of different content of water. The background reaction (dark brown trace) was measured during cooling with 5% water in the feed. Right: Reduction peak edge temperatures from the left panel plotted together with catalytic data for the inhibition from the kinetic experiments at 500 ppm CH<sub>4</sub> in Fig. 4 bottom right.

reaction of water with site S to give an inhibited site S\* (H<sub>2</sub>O) corresponding to water, hydroxyl or similar adsorbed on the site. Eq. 3 is conversion of methane on the inhibited site, which results in complete deactivation and loss of the active site.

Since S\* (H<sub>2</sub>O) responds immediately to changes in the water content, we expect that the rate constants for water adsorption  $k_{2f}$  and desorption  $k_{2r}$  are large. If the dry methane oxidation reaction is kept under 350 °C, a mild deactivation caused by the reaction with product water is observed, see Fig. S14. This indicates that the formed water is also adsorbed on the catalyst's surface at low temperatures.

From Eqs. 1–3, we developed a simple quasi-empirical kinetic model to test our understanding of the deactivation mechanism. Eq. 4 shows a typical Langmuir-Hinshelwood expression that assumes a first order reaction in methane and zero order reaction in the partial pressure of CO<sub>2</sub> and O<sub>2</sub>.

$$r_{CH_4} = K_1 \cdot p(CH_4) \cdot \theta_S \quad (4)$$

Here,  $K_1$  is the rate constant,  $p(CH_4)$  is the partial pressure of methane, and  $\theta_S$  is the fraction of surface-active sites. The rate constant  $K_1$  is given by the following Arrhenius equation:

$$K_1 = A \cdot e^{-\frac{E_A}{RT}} \quad (5)$$

where  $A$  is the preexponential factor, and  $E_A$  is the apparent activation

energy calculated from the experiment given in Fig. S15. Furthermore, inspired by the work of Olsson et al. [13], we expressed the fraction of surface-active sites as a function of time,  $t$  with two components: A fast (time-independent) and a slow (time-dependent) decrease in the fraction of surface-active sites using the following expression:

$$\theta_S(t) = \frac{1}{1 + K_2 \cdot p(H_2O)^{0.25} + K_3 \cdot p(H_2O)^{1.15} \cdot p(CH_4)^{0.85} \cdot t} \quad (6)$$

The exponents on the water and methane partial pressures in Eq. 6 are obtained using the exponents from Fig. 4 bottom left and right by finding the values where the results fall on the best straight lines through origo as judged by the least squares method. For the slow deactivation, the exponents in Eq. 6 for the time dependent part are well determined from the grid of 36 full data sets each with hundreds of data points. For the inhibition part, the data set is much smaller and was obtained at a slightly different temperature. The exponent for the water in the expression is therefore less well determined.

Using the method of lines, we modelled the plug flow reactor in MatLab by a set of ordinary differential equations and fitted the proposed rate expression to our data sets of conversion versus time at 440 °C. More specifically, we divided the reactor volume into 100 sections and fitted  $K_2$  and  $K_3$  simultaneously using the least squares method on 5 datasets; 200, 1000, and 2500 ppm CH<sub>4</sub> with 10% water and 1000 ppm CH<sub>4</sub> with 1% and 5% water. Fig. 7 shows how the resulting

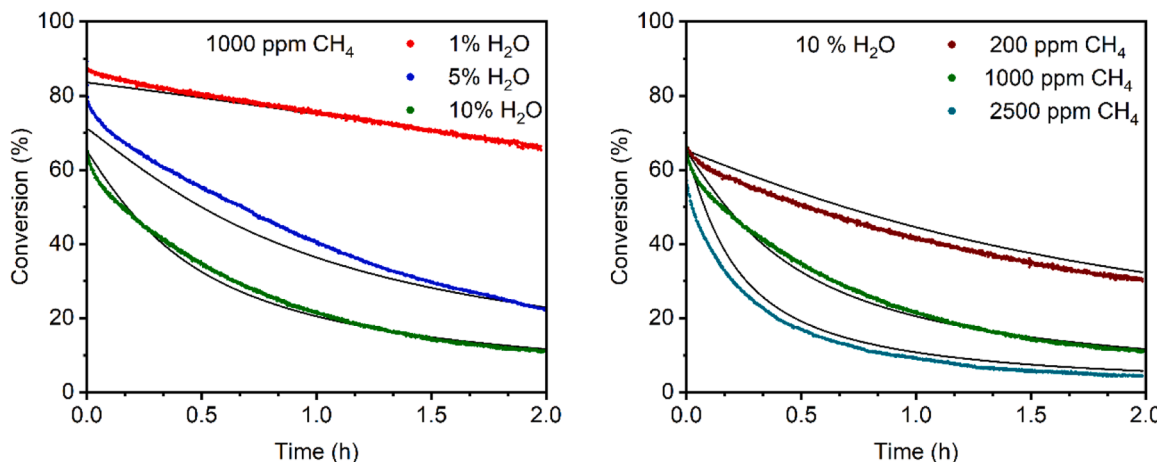


**Fig. 7.** Experimental data of CH<sub>4</sub> conversion vs. time at 440 °C after the water was turned on (colored traces) compared to the predictions of the kinetic model calculated at K<sub>1</sub> = 638 bar<sup>-1</sup> s<sup>-1</sup>, K<sub>2</sub> = 130 bar<sup>-0.25</sup> and K<sub>3</sub> = 410 bar<sup>-2</sup>s<sup>-1</sup> (black traces). Left: 1000 ppm CH<sub>4</sub> together with 1%, 5%, and 10% H<sub>2</sub>O. Right: 10% H<sub>2</sub>O together with 200, 1000, and 2500 ppm CH<sub>4</sub>.

model fits the experimental data and predicts all the general trends in the deactivation under different reaction conditions. Since the proposed model provides a good basis for more advanced modelling, all the data from the kinetic study is available for download in the [Supplementary Material](#).

### 3.5. XAS

We investigated the fresh and spent catalyst by several ex-situ methods, including PXRD, Raman, and DRIFTS. Unfortunately, these methods all showed very small differences between the active and deactivated catalysts (results not shown). Searching for a method with better sensitivity, we investigated the fresh and deactivated sample by X-ray Absorption Spectroscopy (XAS) at the Pd L<sub>3</sub>-edge, see Fig. 8.

The results show that both the fresh and the deactivated sample only contain divalent Pd<sup>2+</sup>, as evidenced by the spectral similarity across the series of samples. Furthermore, the photon energies of the intense resonance ("white line") coincide with that of the PdO reference sample. However, two aspects make the samples' behavior significantly different from the PdO reference. Firstly, the first EXAFS wiggles are broadened compared to PdO suggesting a larger degree of deviation in the local Pd<sup>2+</sup> coordination environment. Secondly, the samples suffered from significant beam-induced deterioration, visualized by the first and sixth

consecutive photon energy scan in Fig. 8. The reference PdO did not experience any visible beam damage at the same measurement conditions.

Comparison of the spectra of the fresh and the deactivated samples show that the deactivated sample has a 27% lower white line integral than the fresh sample. The difference is not related to a difference in oxidation state since the white line photon energy is virtually identical in all three samples and the TPR quantification unequivocally shows that all Pd on both samples are Pd<sup>2+</sup>. Fundamentally, the white line integral is directly related to the number of holes in the 4d levels of Pd and therefore also to the degree of covalency. Empirically, but also recently supported by computational evidence, the Pd L<sub>3</sub>-edge XAS white line integral is lower for a lower average coordination number of Pd expected in smaller PdO particles [30,31].

## 4. Discussion

The fast inhibition by water is well described in the literature [12] and our results corroborate the existing hypothesis: The formation of hydroxyl groups on the surface of the PdO nanoparticles hinders the access of methane and inhibits the initiation of the reaction. The model analysis presented here shows that the best descriptor for the inhibition is the relative rate loss (measured in %) of the methane oxidation reaction. The relative rate loss is independent of the methane content in correspondence with the formation of surface hydroxyl groups. When the water is turned on, the development in the methane conversion follows a softer curve than the sharp turn predicted by the simple model. We tentatively assign this to be due to a short period of establishment of the surface hydroxyl or water coverage in response to the change in water content in the gas phase. In contrast, when the water is turned off, the response is fast as water escapes instantly to the gas phase, see Fig. 1. The relative decrease in rate, Δrate is numerically identical to the relative increase in rate measured after the water is turned off again at both 1, 2, 3 and 4 bar total pressure, see Fig. S10. The change in the reaction rates also follows the edge reduction temperature during CH<sub>4</sub>-TPR very closely showing that both are good descriptors for the inhibition.

The slow deactivation is fundamentally different, and the rate expression depends on both water and methane content, see Fig. 4. Using the 36 independently fitted second order rate coefficients as input, the exponents of the water and methane partial pressures are determined to be 1.15 and 0.85, respectively. Our results further show that the conversion of methane, not just the presence of methane, causes the detrimental effect of water. This is underlined by the fact that the exponent of the partial pressure of methane determined at 440 °C for the

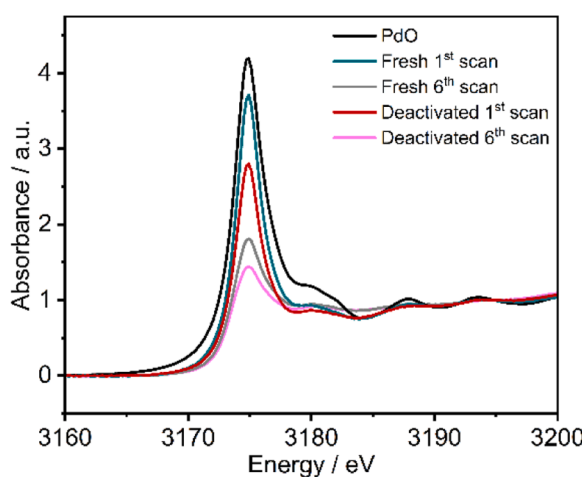


**Fig. 8.** L<sub>3</sub>-edge XAS spectra of the as-prepared fresh catalyst and the deactivated catalyst after wet methane oxidation (1000 ppm CH<sub>4</sub>, 10% O<sub>2</sub>, 10% H<sub>2</sub>O, N<sub>2</sub> balance) for 60 h. The first and sixth scans are shown.

methane oxidation reaction and for the deactivation process is empirically found to be the same: 0.85.

A potential explanation for 1) the lower catalytic reactivity, 2) the delayed reduction by methane in TPR, and 3) the reduced white line integral in XAS of the deactivated catalyst compared to the fresh catalyst is that the morphology of the active PdO particles changes during the reaction. We suggest that the fresh sample has larger nanoparticles and fewer interactions with the support than the deactivated catalyst and that the morphology changes dynamically in response to changes in the experimental conditions. The dispersion of Pd on the alumina surface has been shown to be relevant at above 600–700 °C in a dry oxidizing feed,[32] and water has been shown to also increase dispersion [28]. We suggest that dispersion is the main reason for the slow deactivation in wet methane oxidation at temperatures below 550 °C. Our hypothesis is in correspondence with the following experimental observations:

- 1) Highly dispersed palladium is less active than agglomerated particles in the methane oxidation reaction [14,32,33].
- 2) Highly dispersed palladium is observed to have a significantly higher reduction temperature in TPR [34].
- 3) Highly dispersed and therefore on average smaller palladium oxide particles are expected to have a lower white line integral in L<sub>3</sub>-edge XAS compared to larger particles due to a smaller average coordination number [30].

The effect is completely reversed by exposing the catalyst to reducing conditions, see Fig. S12, and therefore the hypothesis implicates a hypothesis of ripening or agglomeration at reducing conditions. A similar dispersion-assembly mechanism has previously been suggested for Pd in zeolites [35] and for the closely related Pt on CeO<sub>2</sub> [36] and MgAlO<sub>4</sub> [37]. In these cases, oxidizing conditions also facilitates dispersion, while reducing conditions facilitates ripening or agglomeration. The exact manner of dispersion is still not fully understood. We hypothesize that the methane oxidation activity is lost when the dimensions of the parent active PdO particles decrease below a certain critical level. This could be either formation of smaller particles or it could be flattening of the original spherical particles. We expect the extent of dispersion to be very dependent on the support material.

With this hypothesis, the experimental observations can be rationalized. Dispersed Pd<sup>2+</sup> is hypothesized to be the endpoint at wet methane oxidation conditions and more energetically favored at these conditions. Clustered metallic Pd<sup>0</sup> is energetically favored at reducing conditions and the agglomeration is observed to happen very fast. The oxidation of methane to CO<sub>2</sub> requires Pd<sup>0</sup> to be oxidized to PdO first to allow the Mars van Krevelen-type mechanism, where PdO supplies the O atoms to both CO<sub>2</sub> and H<sub>2</sub>O [29,38]. Each methane molecule will require 4 oxygens corresponding to an increase in oxidation state of carbon of 8 and the generation of 4 Pd<sup>0</sup>. The oxidation is shown by several groups to proceed faster if Pd<sup>0</sup> is also present and it is suggested to be the site where methane absorbs and the first and most difficult C-H bond breaks [38,39]. Reoxidation of Pd<sup>0</sup> by dioxygen have a higher onset temperature than reduction of PdO by methane at both dry and wet conditions [29] and is assumed to follow the Cabrera-Mott mechanism [17]. During methane oxidation the reduction of PdO by methane and the oxidation of Pd<sup>0</sup> by dioxygen are competing. Therefore, it can be envisioned that a methane oxidation event results in the formation of a transient Pd<sup>0</sup> region on the PdO surface as described by Bell et. al. [38] It has only a limited lifetime before it is reoxidized by the excess O<sub>2</sub>. During this short but significant time window, the coexisting Pd<sup>0</sup> and PdO ensures high catalytic activity.

Our hypothesis implies that Pd<sup>0</sup> is very mobile under realistic operation since a short reducing pulse results in full regeneration. A transient Pd<sup>0</sup> region of the active nanoparticles formed during operation is consequently also suggested to be very mobile. There will be an entropic driving force for the Pd<sup>0</sup> area to migrate to or beyond the edge of the parent PdO particle. The endpoint after migration and reoxidation is

dispersed Pd<sup>2+</sup>, which is more difficult to reduce and therefore less catalytically active and, according to the hypothesis, also less mobile. Eventually, more and more Pd will be trapped in a catalytically dead dispersed state. The formation of this inactive state is connected to the conversion of methane in accordance with our observations. The inactive state of Pd can be released again by a short reducing pulse, i.e. by shifting for a few seconds to rich operation or by increasing the temperature until methane reduces Pd and allows re-agglomeration of Pd and regeneration of the catalyst. Water is important for deactivating the catalyst in at least two separate ways. It hinders the reduction of palladium by methane by covering the PdO surface with hydroxyl groups giving fewer highly active sites which consists of both Pd<sup>0</sup> and PdO [33] and it aids in trapping Pd<sup>2+</sup> on a support surface site by stabilizing the dispersed Pd<sup>2+</sup> [32]. At dry methane oxidation conditions only the water generated by the reaction is available and the deactivation is less severe.

The support material is decisive in methane oxidation catalysis. On one hand, it should allow quite high dispersion of Pd to have a high surface area of palladium. PdO particles above 3–5 nm have lower activity due to inaccessible bulk atoms. On the other hand, too high dispersion is detrimental for the activity.

## 5. Conclusion

We have shown that the deactivation of a PdO/Al<sub>2</sub>O<sub>3</sub> catalyst under realistic methane oxidation operation conditions is composed of two separate phenomena, a fast reversible inhibition of the active sites and a slow, irreversible loss of the active sites. Both phenomena significantly increase the reduction temperature of Pd<sup>2+</sup> as probed by CH<sub>4</sub>-TPR, and the observed shift of reduction temperature is an excellent descriptor for the degree of deactivation. Furthermore, the increase in reduction temperature and the change in reduction profile of all Pd present indicates that the slow deactivation is not a surface phenomenon on PdO particles but a change in morphology of the Pd phase. The slow deactivation occurs when methane is converted under oxidizing conditions in the presence of water. The deactivation can always be reversed instantly and reproducibly through a short reductive treatment. Based on a comprehensive kinetic study, we propose three reaction equations and a simple quasi-empirical kinetic model that captures the key trends in the catalytic deactivation over time under the different reaction conditions.

After long reaction time in wet reaction conditions, the deactivated sample is only subtly different from the fresh catalyst and several typical characterization methods fail to show a significant difference, possibly due to the low concentration of PdO on the support. The best method to distinguish and quantify the phase changes and study both inhibition and deactivation with excellent resolution is the newly developed CH<sub>4</sub>-TPR methodology. The high mobility of Pd<sup>0</sup> at elevated temperatures makes it challenging to investigate the dispersion [33]. This is important as a take-home message as many groups routinely treat their samples in hydrogen at elevated temperatures to have a reproducible state before e.g. chemisorption or spectroscopic analysis but this treatment will change the composition of the surface Pd phase and is not useful for investigating the result of deactivation.

Based on our findings, we confirm that hydroxyl or water coverage causes the fast inhibition and propose that water facilitates dispersion of Pd on the support during methane oxidation and that this is observed as irreversible slow deactivation of the catalyst.

## CRediT authorship contribution statement

**Pedersen Kim:** Conceptualization, Funding acquisition, Project administration, Resources, Supervision. **Noack Hendrik-David:** Methodology, Resources, Supervision. **Pedersen Kasper Steen:** Investigation, Resources. **Dunstan Maja A.:** Data curation, Investigation. **Rogalev Andrei:** Methodology, Resources. **Wilhelm Fabrice:** Data

curation, Investigation. **Mossin Susanne**: Conceptualization, Funding acquisition, Methodology, Project administration, Resources, Supervision, Writing – review & editing. **Mielby Jerrik**: Conceptualization, Investigation, Methodology, Project administration, Supervision, Writing – review & editing, Resources. **Mortensen Rasmus Lykke**: Data curation, Formal analysis, Investigation, Methodology, Writing – original draft, Writing – review & editing, Visualization.

## Declaration of Competing Interest

The authors declare the following financial interests/personal relationships which may be considered as potential competing interests: Susanne Mossin and Kim Pedersen reports financial support was provided by Innovation Fund Denmark. Susanne Mossin reports financial support was provided by Carlsberg Foundation. Kim Pedersen, Hendrik-David Noack and Rasmus L. Mortensen reports a relationship with Umicore Denmark ApS that includes: employment.

## Data availability

Kinetic data file is available for download as an excel file.

[ESI\\_kinetic data.xlsx \(Original data\)](#) (DTU Data)

## Acknowledgements

This work was funded by Umicore Denmark and Innovation Fund Denmark (IFD) under File No. 0153-00064B. Carlsberg Foundation is acknowledged for supporting infrastructure under CF19-0367. We are grateful to Prof. Avelino Corma and Dr. Ton V.W. Janssens for fruitful discussions.

## Appendix A. Supporting information

Additional figures and detailed descriptions of experiments are available for download as a pdf file and can be downloaded free of charge from the journal homepage. Kinetic data is available for download as an excel file from the DTU data repository: <https://data.dtu.dk/>. Supplementary data associated with this article can be found in the online version at [doi:10.1016/j.apcatb.2023.123646](https://doi.org/10.1016/j.apcatb.2023.123646).

## References

- [1] D.L. Mowery, R.L. McCormick, Deactivation of alumina supported and unsupported PdO methane oxidation catalyst: the effect of water on sulfate poisoning, *Appl. Catal. B* 34 (2001) 287–297, [https://doi.org/10.1016/S0926-3373\(01\)00222-3](https://doi.org/10.1016/S0926-3373(01)00222-3).
- [2] P. Losch, W. Huang, O. Vozniuk, E.D. Goodman, W. Schmidt, M. Cargnello, Modular Pd/zeolite composites demonstrating the key role of support hydrophilic/hydrophilic character in methane catalytic combustion, *ACS Catal.* 9 (2019) 4742–4753, <https://doi.org/10.1021/acscatal.9b00596>.
- [3] A.W. Petrov, D. Ferri, O. Kröcher, J.A. Van Bokhoven, Design of stable palladium-based zeolite catalysts for complete methane oxidation by postsynthesis zeolite modification, *ACS Catal.* 9 (2019) 2303–2312, <https://doi.org/10.1021/acscatal.8b04486>.
- [4] H. Hosseiniamoli, A. Setiawan, A.A. Adesina, E.M. Kennedy, M. Stockenhuber, The stability of Pd/TS-1 and Pd/silicalite-1 for catalytic oxidation of methane—understanding the role of titanium, *Catal. Sci. Technol.* 10 (2020) 1193–1204, <https://doi.org/10.1039/c9cy01579e>.
- [5] I. Friberg, N. Sadokhina, L. Olsson, The effect of Si/Al ratio of zeolite supported Pd for complete CH<sub>4</sub> oxidation in the presence of water vapor and SO<sub>2</sub>, *Appl. Catal. B* 250 (2019) 117–131, <https://doi.org/10.1016/j.apcatb.2019.03.005>.
- [6] R.L. Mortensen, H. Noack, K. Pedersen, S. Mossin, J. Mielby, Recent advances in complete methane oxidation using zeolite-supported metal nanoparticle catalysts, *ChemCatChem* 14 (2022) e2021019, <https://doi.org/10.1002/cctc.202101924>.
- [7] X. Li, X. Wang, K. Roy, J.A. van Bokhoven, L. Artiglia, Role of water on the structure of palladium for complete oxidation of methane, *ACS Catal.* 10 (2020) 5783–5792, <https://doi.org/10.1021/acscatal.0c01069>.
- [8] Y. Zhang, P. Glarborg, M.P. Andersson, K. Johansen, T.K. Torp, A.D. Jensen, J. M. Christensen, Influence of the support on rhodium speciation and catalytic activity of rhodium-based catalysts for total oxidation of methane, *Catal. Sci. Technol.* 10 (2020) 6035–6044, <https://doi.org/10.1039/D0CY00847H>.
- [9] K. Murata, J. Ohyama, Y. Yamamoto, S. Arai, A. Satsuma, Methane combustion over Pd/Al2O3 Catalysts in the presence of water: effects of Pd particle size and alumina crystalline phase, *ACS Catal.* 10 (2020) 8149–8156, <https://doi.org/10.1021/acscatal.0c02050>.
- [10] R. Gholami, M. Alyani, K. Smith, Deactivation of Pd catalysts by water during low temperature methane oxidation relevant to natural gas vehicle converters, *Catalysts* 5 (2015) 561–594, <https://doi.org/10.3390/catal5020561>.
- [11] D. Ciuparu, E. Perkins, L. Pfefferle, In situ DR-FTIR investigation of surface hydroxyls on γ-Al 2O3 supported PdO catalysts during methane combustion, *Appl. Catal. A Gen.* 263 (2004) 145–153, <https://doi.org/10.1016/j.apcata.2003.12.006>.
- [12] P. Velin, F. Hemmingsson, A. Schaefer, M. Skoglundh, K.A. Lomachenko, A. Raj, D. Thompsett, G. Smedler, P. Carlsson, Hampered PdO redox dynamics by water suppresses lean methane oxidation over realistic palladium catalysts, *ChemCatChem* 13 (2021) 3765–3771, <https://doi.org/10.1002/cctc.202100829>.
- [13] N. Sadokhina, F. Ghasempour, X. Auvray, G. Smedler, U. Nyblén, M. Olofsson, L. Olsson, An experimental and kinetic modelling study for methane oxidation over Pd-based catalyst: inhibition by water, *Catal. Lett.* 147 (2017) 2360–2371, <https://doi.org/10.1007/s10562-017-2133-2>.
- [14] P. Velin, C.R. Florén, M. Skoglundh, A. Raj, D. Thompsett, G. Smedler, P. A. Carlsson, Palladium dispersion effects on wet methane oxidation kinetics, *Catal. Sci. Technol.* 10 (2020) 5460–5469, <https://doi.org/10.1039/d0cy00734j>.
- [15] M. Roger, O. Kröcher, D. Ferri, Assessing the effect of O<sub>2</sub> dithering on CH<sub>4</sub> oxidation on Pd/Al2O3, *Chem. Eng. J.* 451 (2022) 138865, <https://doi.org/10.1016/j.cej.2022.138865>.
- [16] F. Arosio, S. Colussi, A. Trovarelli, G. Groppi, Effect of alternate CH<sub>4</sub>-reducing/lean combustion treatments on the reactivity of fresh and S-poisoned Pd/CeO<sub>2</sub>/Al2O3 catalysts, *Appl. Catal. B* 80 (2008) 335–342, <https://doi.org/10.1016/j.apcatb.2007.11.030>.
- [17] T. Franken, M. Roger, A.W. Petrov, A.H. Clark, M. Agote-Arán, F. Krumeich, O. Kröcher, D. Ferri, Effect of short reducing pulses on the dynamic structure, activity, and stability of Pd/Al 2 O 3 for wet lean methane oxidation, *ACS Catal.* 11 (2021) 4870–4879, <https://doi.org/10.1021/acscatal.1c00328>.
- [18] A.W. Petrov, D. Ferri, F. Krumeich, M. Nachtegaal, J.A. van Bokhoven, O. Kröcher, Stable complete methane oxidation over palladium based zeolite catalysts, *Nat. Commun.* 9 (2018) 2545, <https://doi.org/10.1038/s41467-018-04748-x>.
- [19] A. Boucly, L. Artiglia, M. Roger, M. Zabilskiy, A. Beck, D. Ferri, J.A. van Bokhoven, Water inhibition and role of palladium adatoms on Pd/Al2O3 catalysts during methane oxidation, *Appl. Surf. Sci.* 606 (2022) 154927, <https://doi.org/10.1016/j.apsusc.2022.154927>.
- [20] J. Nilsson, P.-A. Carlsson, N.M. Martin, E.C. Adams, G. Agostini, H. Grönbeck, M. Skoglundh, Methane oxidation over Pd/Al2O3 under rich/lean cycling followed by operando XAFS and modulation excitation spectroscopy, *J. Catal.* 356 (2017) 237–245, <https://doi.org/10.1016/j.jcat.2017.10.018>.
- [21] K.I. Shimizu, Y. Kamiya, K. Osaki, H. Yoshida, A. Satsuma, The average Pd oxidation state in Pd/SiO<sub>2</sub> quantified by L 3-edge XANES analysis and its effects on catalytic activity for CO oxidation, *Catal. Sci. Technol.* 2 (2012) 767–772, <https://doi.org/10.1039/c2cy00422d>.
- [22] A.W. Petrov, D. Ferri, M. Tarik, O. Kröcher, J.A. van Bokhoven, Deactivation aspects of methane oxidation catalysts based on palladium and ZSM-5, *Top. Catal.* 60 (2017) 123–130, <https://doi.org/10.1007/s11244-016-0724-6>.
- [23] X. Li, X. Wang, K. Roy, J.A. van Bokhoven, L. Artiglia, Role of water on the structure of palladium for complete oxidation of methane, *ACS Catal.* 10 (2020) 5783–5792, <https://doi.org/10.1021/acscatal.0c01069>.
- [24] P. Velin, M. Ek, M. Skoglundh, A. Schaefer, A. Raj, D. Thompsett, G. Smedler, P. A. Carlsson, Water inhibition in methane oxidation over alumina supported palladium catalysts, *J. Phys. Chem. C* 123 (2019) 25724–25737, <https://doi.org/10.1021/acs.jpcc.9b07606>.
- [25] K. Keller, P. Lott, H. Stotz, L. Maier, O. Deutschmann, Microkinetic modeling of the oxidation of methane over pdo catalysts-towards a better understanding of the water inhibition effect, *Catalysts* 10 (2020) 1–21, <https://doi.org/10.3390/catal10080922>.
- [26] L. Zhang, J. Chen, X. Guo, S. Yin, M. Zhang, Z. Rui, Combination of reduction-deposition Pd loading and zeolite dealumination as an effective route for promoting methane combustion over Pd/Beta, *Catal. Today* 376 (2020) 119–125, <https://doi.org/10.1016/j.cattod.2020.07.005>.
- [27] W. Wang, W. Zhou, W. Li, X. Xiong, Y. Wang, K. Cheng, J. Kang, Q. Zhang, Y. Wang, In-situ confinement of ultrasmall palladium nanoparticles in silicalite-1 for methane combustion with excellent activity and hydrothermal stability, *Appl. Catal. B* 276 (2020) 119142, <https://doi.org/10.1016/j.apcatb.2020.119142>.
- [28] A. Boucly, L. Artiglia, M. Roger, M. Zabilskiy, A. Beck, D. Ferri, J.A. van Bokhoven, Water inhibition and role of palladium adatoms on Pd/Al2O3 catalysts during methane oxidation, *Appl. Surf. Sci.* 606 (2022) 154927, <https://doi.org/10.1016/j.apsusc.2022.154927>.
- [29] E.D. Goodman, A.A. Ye, A. Aitbekova, O. Mueller, A.R. Riscoe, T. Nguyen Taylor, A.S. Hoffman, A. Boubnov, K.C. Bustillo, M. Nachtegaal, S.R. Bare, M. Cargnello, Palladium oxidation leads to methane combustion activity: effects of particle size and alloying with platinum, *J. Chem. Phys.* 151 (2019) 154703, <https://doi.org/10.1063/1.5126219>.
- [30] M.W. Tew, J.T. Miller, J.A. Van Bokhoven, Particle size effect of hydride formation and surface hydrogen adsorption of nanosized palladium catalysts: L3 Edge vs K Edge X-ray absorption spectroscopy, *J. Phys. Chem. C* 113 (2009) 15140–15147, <https://doi.org/10.1021/jp902542f>.
- [31] J. Nilsson, P.-A. Carlsson, H. Grönbeck, M. Skoglundh, First principles calculations of palladium nanoparticle XANES spectra, *Top. Catal.* 60 (2017) 283–288, <https://doi.org/10.1007/s11244-016-0612-0>.

- [32] E.D. Goodman, A.C. Johnston-Peck, E.M. Dietze, C.J. Wrasman, A.S. Hoffman, F. Abild-Pedersen, S.R. Bare, P.N. Plessow, M. Cargnello, Catalyst deactivation via decomposition into single atoms and the role of metal loading, *Nat. Catal.* 2 (2019) 748–755, <https://doi.org/10.1038/s41929-019-0328-1>.
- [33] Y. Cui, J. Zhu Chen, B. Peng, L. Kovarik, A. Devaraj, Z. Li, T. Ma, Y. Wang, J. Szanyi, J.T. Miller, Y. Wang, F. Gao, Onset of high methane combustion rates over supported palladium catalysts: from isolated Pd cations to PdO nanoparticles, *JACS Au* 1 (2021) 396–408, <https://doi.org/10.1021/jacsau.0c00109>.
- [34] T.M. Lardinois, J.S. Bates, H.H. Lippie, C.K. Russell, J.T. Miller, H.M. Meyer, K. A. Unocic, V. Prikhodko, X. Wei, C.K. Lambert, A.B. Getsoiyan, R. Gounder, Structural interconversion between agglomerated palladium domains and mononuclear Pd(II) cations in chabazite zeolites, *Chem. Mater.* 33 (2021) 1698–1713, <https://doi.org/10.1021/acs.chemmater.0c04465>.
- [35] B.J. Adelman, W.M.H. Sachtler, The effect of zeolitic protons on NO(x) reduction over Pd/ZSM-5 catalysts, *Appl. Catal. B* 14 (1997) 1–11, [https://doi.org/10.1016/S0926-3373\(97\)00007-6](https://doi.org/10.1016/S0926-3373(97)00007-6).
- [36] M. Farnesi Camellone, F. Dvořák, M. Vorokhta, A. Tovt, I. Khalakhan, V. Johánek, T. Skála, I. Matolínová, S. Fabris, J. Mysliveček, Adatom and nanoparticle dynamics on single-atom catalyst substrates, *ACS Catal.* 12 (2022) 4859–4871, <https://doi.org/10.1021/acscatal.2c00291>.
- [37] D. Chakraborty, T.E.L. Smitshuysen, A. Kakekhani, S.P.F. Jespersen, S. Banerjee, A. Krabbe, N. Hagen, H. Silva, J. Just, C.D. Damsgaard, S. Helveg, A.M. Rappe, J. K. Nørskov, I. Chorkendorff, Reversible atomization and nano-clustering of Pt as a strategy for designing ultra-low-metal-loading catalysts, *J. Phys. Chem. C* 126 (2022) 16194–16203, <https://doi.org/10.1021/acs.jpcc.2c05213>.
- [38] S.C. Su, J.N. Carstens, A.T. Bell, A study of the dynamics of Pd oxidation and PdO reduction by H<sub>2</sub> and CH<sub>4</sub>, *J. Catal.* 176 (1998) 125–135, <https://doi.org/10.1006/jcat.1998.2028>.
- [39] A. Hellman, A. Resta, N.M. Martin, J. Gustafson, A. Trinchero, P.A. Carlsson, O. Balmes, R. Felici, R. Van Rijn, J.W.M. Frenken, J.N. Andersen, E. Lundgren, H. Grönbeck, The active phase of palladium during methane oxidation, *J. Phys. Chem. Lett.* 3 (2012) 678–682, <https://doi.org/10.1021/jz300069s>.